Measurement and Modeling of Duty-Cycle Effects Due to NBTI

K. E. Kambour[o], D. D. Nguyen*, C. Kouhestani* and R. A. B. Devine[#]
[o]SAIC, *COSMIAC, [#]Think-Strategically
Air Force Research Laboratory, Space Vehicles Directorate
Kirtland AFB, NM USA

***Abstract*— One of the most important requirements for modeling of the long-term effects of negative bias temperature instability (NBTI) on device/circuit response is an understanding of how to include the effect of duty cycle on the threshold voltage shift. Since NBTI is known to be comprised of both permanent and recoverable components, a measurement protocol must be established enabling separation of these components and then their recombination to predict the shift for different duty cycles. In the work reported here, we have endeavored to address these issues by combining pulsed and pseudo-DC stressing/relaxation methods.**

I. Introduction

The need to maintain device reliability greater than ten years for space-based applications has led to greater interest into the fundamental mechanisms of device/circuit failure. One of the most important of these mechanisms is negative bias temperature instability (NBTI) in which the threshold voltage, V_{th}, of a p-channel metal oxide semiconductor (PMOS) increases in magnitude due to the application of a negative bias on the gate and then partially recovers over time after the bias is removed.

The desire to model the long-term effects of NBTI on device/circuit response using accelerated testing of devices requires the development of an understanding of how to include duty cycle, D (defined as the time the device is under negative bias stressing divided by the total time), effects [1-3] on ΔV_{th}. NBTI in nitrided SiO_2 is known to be comprised [4] of multiple components, some permanent (defined here as those that do not recover in a reasonable time at zero bias conditions) and others recoverable, each of which may have a different dependence on duty cycle. Given this, a measurement protocol must be developed enabling separation of the individual components and their time dependencies. The eventual goal is to develop the ability to predict the total ΔV_{th} of a device over a range of duty cycles which may then be used in a circuit simulation to predict the behavior of the circuit over long times.

II. Experimental measurements

All measurements were carried out using a Keithley Instruments Inc. 4200-SCS Semiconductor Characterization System. The metal-oxide-semiconductor field effect transistor (MOSFET) devices studied were 130 nm channel length by 5 μm channel width with 3.4-nm thick nitrided SiO_2 gate insulators. For the experiments described, the devices were heated to 120° C and then measurements were made in the measure/stress(or relax)/measure mode with the gate voltage, V_{gs}, ramped from the stressing (relaxation) voltage, V_{gs}(stress) or V_{gs}(relax), to the measurement voltage, V_{gs}(meas.), in ~ 20 ns. V_{gs}(meas.) was typically – 0.52 V and ascertained to be the voltage of maximum dI_{ds}/dV_{gs} on the $I_{ds}(V_{gs})$ curve obtained at small V_{ds}. Source/drain current, I_{ds}, was measured in ~ 4 μs with a drain/source voltage of – 50 mV. During stressing the voltage on the gate, V_{gs}(stress), was chosen to be -3.25 V whilst the source/drain/body contacts were shorted. For relaxation studies, V_{gs}(relax) was either 0 V or + 1.5 V. A pulsed stressing approach was employed in which the pulse repetition frequency was in the range 10 Hz to 100 kHz, and the duty cycle was in the range of 0 to 1 – the latter corresponded to a pseudo-DC measurement. A typical representation of the time variation of V_{gs} employed is shown in Fig. 1. For the "AC" pulsed stress/measurement I_{ds} could be measured either following the V_{gs}(stress) component of the final pulse (Fig. 1b) or following V_{gs}(relax) part of the pulse (Fig. 1c). The relevance of these modes of measurement will become evident in the following.

Using the pseudo-DC mode of stress/measurement, we determined [5] that at least three "species" of charging contribute to the electrical stress-induced variation of the threshold voltage shift, $\Delta V_{th}(t_{stress})$. These components are: a) ΔV_{th}(RC) resulting from dynamic charging/discharging that

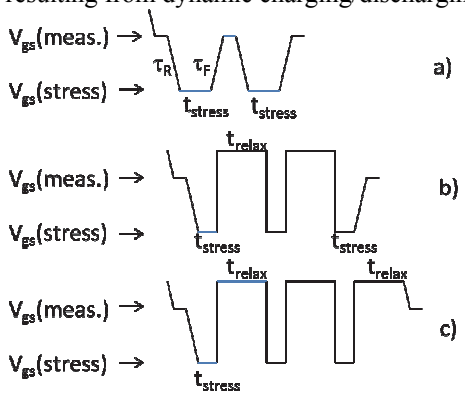

Fig. 1: The three voltage-pulse sequences used in this research. For the DC pulse measurement , (a) the gate bias is constant for a time, t_{stress}, and then the gate bias is reduced to measure the source-drain current before being returned to the stressing level. $\tau_R \sim \tau_F \sim 20$ ns. The "AC" sequences are shown in (b) and (c). Many stress and relaxation cycles are applied before the measurement is made. This is performed either immediately following a stress part (b) or relaxation part (c) of the final pulse.

978-1-4673-2752-7/12/$31.00 ©2012 IEEE

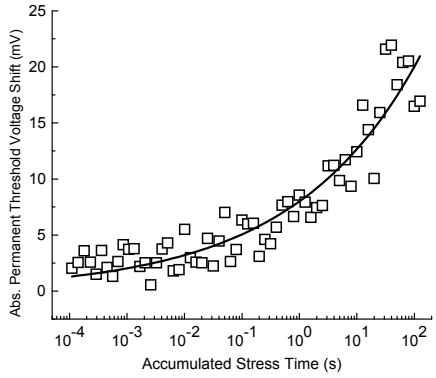

Fig. 2: The measured growth of the permanent component of the threshold voltage shift ($\Delta V_{th}(IS) + \Delta V_{th}(FRC)$) as a function of total stress time (squares) and the fitted form $\Delta V_{th}=At^{\alpha}$ where A=8 mV and α =0.2.

can be repeatedly cycled and relaxes under V_{gs} = 0 V, b) $\Delta V_{th}(FRC)$ a field recoverable charging which only recovers in the presence of a positive bias on V_{gs} and c) $\Delta V_{th}(IS)$ due primarily to permanently charged interface states, though permanently charged oxide traps cannot be excluded. Starting with a duty cycle of 0.1 to pulse stress devices, we observed that following V_{gs}(relax) at 0 V there was full recovery of the RC component, and the remaining ΔV_{th} was therefore equal to the sum of ($\Delta V_{th}(IS) + \Delta V_{th}(FRC)$). The variation of this term with stress time was fitted using a law of the form ($\Delta V_{th}(IS) + \Delta V_{th}(FRC)$) = At^{α}_{stress}. We then performed a series of experiments in which the duty cycle was varied and fits were made assuming At^{α}_{stress}. We ascertained the limits of the duty cycle within which there was no change in A or α. A typical plot of the permanent components $\Delta V_{th}(IS) + \Delta V_{th}(FRC)$ as a function of total accumulated stress time is shown in Fig. 2. This data can be fitted using $\alpha \sim 0.2$ and A = 8 mV. If this process is repeated but with relaxation at V_{gs}=+1.5 V, it is possible to obtain $\Delta V_{th}(IS)$ alone, in which case we find $\alpha \sim$ 0.3 and A = 6 mV. The α value in this case is consistent with the work of Grasser and co-workers [6].

By taking the $\Delta V_{th}(t_{stress})$ for a pseudo-DC measurement such as shown in Fig. 3 and subtracting the combined permanent component ($\Delta V_{th}(IS) + \Delta V_{th}(FRC)$) as a function of

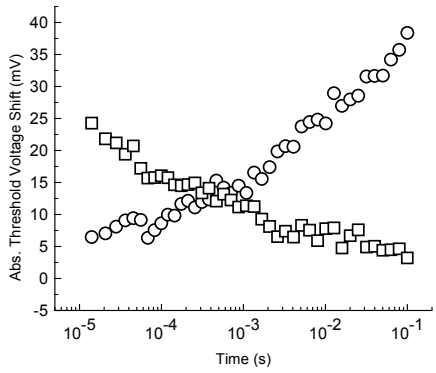

Fig. 3: The measured charging (○) and relaxation (□) of the total threshold voltage shift ($\Delta V_{th}(IS) + \Delta V_{th}(FRC)+\Delta V_{th}(RC)$).

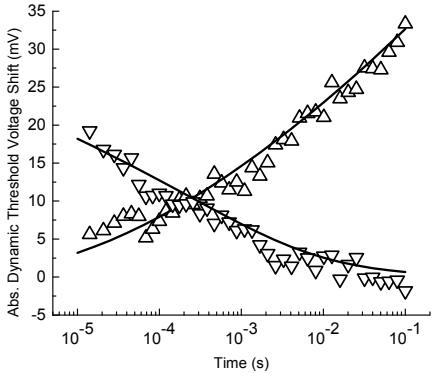

Fig. 4: The measured (points) and fitted (lines) for charging (△) and relaxation (▽) of the dynamic component of the threshold voltage shift ($\Delta V_{th}(RC)$). The fitting of each is based on the Tewksbury formalism [7].

stress time fitted earlier, it is possible to extract $\Delta V_{th}(RC)(t_{stress})$. Then assuming that there is no recovery in ($\Delta V_{th}(IS) + \Delta V_{th}(FRC)$) during the relaxation phase (for example, of Fig. 3), one can determine $\Delta V_{th}(RC)$)(t_{relax}). The charging and recovery as a function of time of $\Delta V_{th}(RC)$ is then determined as shown in Fig. 4.

III. MODELING

The recoverable charge shown in Fig. 4 for a 100 ms stress followed by a 100 ms relaxation was modeled using a version of the Tewksbury formalism [7]. It should be underlined that it has been argued that the Tewksbury model per se is not physically correct to describe the mechanism responsible for $\Delta V_{th}(RC)$ [6]. We have employed it as a convenient mathematical description which would give us the observed dependence of $\Delta V_{th}(RC)$ on both log(t) and $\log^2(t)$ without the intent to imply its applicability as a physical model.

To fit the experimental charging, code was written to numerically integrate

$$\Delta V_{th}(RC)=B_1\int_0^{t_{ox}}(1-e^{-t/\tau_S(x)})dx+ B_2\int_0^{t_{ox}}x(1-e^{-t/\tau_S(x)})dx \quad (1)$$

where t_{ox} is the gate oxide thickness and $\tau_s=\tau_{os}e^{k_s x}$. The corresponding recovery is then given by

$$\Delta V_{th}(RC)=B_1\int_0^{t_{ox}}(1-e^{-t_S/\tau_S(x)})e^{-t/\tau_r(x)}dx + B_2\int_0^{t_{ox}}x(1-e^{t_S/\tau_S(x)})\,e^{-t/\tau_r(x)}dx \quad (2)$$

where $\tau_r = \tau_{or}e^{k_r x}$. This meant that for the charging the fitting parameters were B_1, B_2, τ_{os} and k_s, while for the recovery the adjustable parameters were τ_{or} and k_r. The fit shown in Fig. 4 can clearly be usefully employed to predict the stress time and relaxation time dependence of $\Delta V_{th}(RC)$ whatever physical incorrectness it possesses.

The code as written is also capable of including the growth of the permanent terms and to allow the summation of a series of cycles in order to predict the total threshold voltage shift as a function of time for a given duty cycle and frequency. In order to do this, it is necessary to track the charge left after the relaxation pulse and then allow the next stress and relaxation

cycle to deposit new charge while allowing for some relaxation of all the charge deposited. To accomplish this, a recursion relationship was developed such that the already-charged traps at each depth in the material were removed from the available trap density to be charged at that depth by the new stress. Once the density of newly charged traps was determined, the pre-existing charge was added. Exponential relaxation was then allowed to occur on all trapped charge. Using this approach, it was then possible to add up the charge deposited in thousands and even millions of cycles.

IV. Duty Cycle

We measured the duty cycle dependence of the NBTI effect in our devices. For this purpose, the duty cycle was adjusted between 0 and 1 and the total time was chosen as 500 seconds so that for a given duty cycle the stress time = duty cycle x total time. The experimental data is shown in Fig. 5.

The experimental charging/relaxation data in Fig. 4 appears to show a relaxation rate in ΔV_{th}(RC) that far exceeds the charging rate. In consequence, one would expect the measured (ΔV_{th}(IS) + ΔV_{th}(FRC)) to be the only relevant term in Fig. 5 (shown by the dashed line). However, the experimental data for the duty cycle measurement shows evidence for a significant cycle to cycle build up even for a duty cycle of 0.5. This seeming contradiction in the data is perplexing. It would suggest that over many cycles there is a growth in charge density, presumably "deep" in the dielectric, which relaxes slower than it charges and is not anticipated in the Tewksbury formalism. We have been able to simulate this effect by allowing the charging and discharging terms described by Eqs. 1 and 2 to have different values of k_s and k_r. The discharging of the recoverable charge can in fact be fit using a wide range of k_r and τ_{or} pairs, but to match both the duty cycle and DC charging, only one pair is possible with the fit shown in Fig. 5.

V. Analysis

The effect of the duty cycle on the threshold voltage shift can be divided into three regions in our devices based on this analysis. In the low duty cycle region, < ~0.15, the time dependence of ΔV_{th} is simply that of the permanent charging with the recoverable charge fully discharging before the next cycle begins as can be seen in the similarity between the

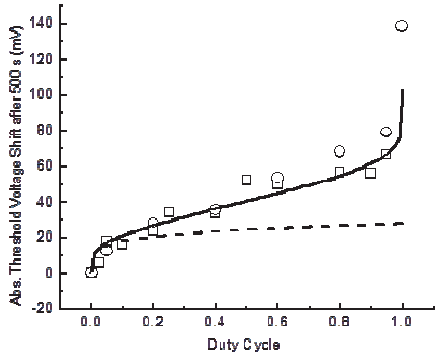

Fig. 5: The magnitude of the threshold voltage shift, ΔV_{th}, after a total time of 500 seconds as a function of duty cycle. The experimental data was taken at 10 Hz (○) and 10 kHz (□). The solid line is the result of simulation at 10Hz. The dashed curve is the simulation result if there is no recoverable charging.

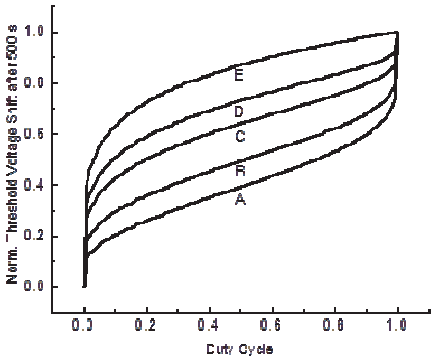

Fig. 6: The predicted normalized threshold voltage shift assuming the dynamic charging is 100% (A), 50% (B), 20% (C), 10% (D), and 0% (E) of the fitted value for our devices.

dashed and solid lines in Fig. 5. In the middle region, 0.15 <duty cycle <0.9, there is a linear increase in threshold voltage as a function of duty cycle which is followed by a rapid upswing at very high duty cycles. In retrospect, this is not surprising since the discharge depends on the log(t). This means that the amount of charge discharged during a wide range of duty cycles is nearly the same, so the difference depends largely on how long the recoverable charge component grows.

The modeling can be used to study the importance of the relative magnitude of the recoverable charge term. This is particularly important as the level of recoverable charge could vary substantially with process flow/materials used in the gate dielectric. In contrast, the density of interface states is relatively constant and the size of the field recoverable term is often small. For this reason calculations were performed in which B_1 and B_2 were reduced in order to see the effect on the duty cycle plot. As can be seen in Fig. 6, the S shape of the curve is more pronounced for higher levels of recoverable charge but eventually shows a smooth growth curve, thus explaining the variance in the shapes seen by others [8]. Note that for simplicity of representation we have normalized all the curves to unity for a duty cycle of 1 [8].

As shown in Figs. 5 and 7 there is frequency independence of ΔV_{th} (duty cycle, t_{total} = 500s) at least for the situation (Fig. 1c) where measurement is made immediately following the

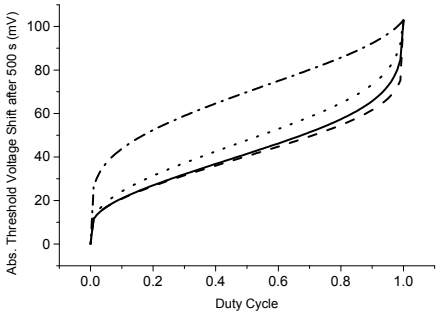

Fig. 7: The predicted threshold voltage shift as a function of duty cycle for f=10kHz if the measurement is taken after relaxation (solid curve) or stress (dotted curve) (Fig. 1b and 1c) and at 10 Hz if the measurement is taken after relaxation (dashed curve) or stress (dotted curve).

final relaxation part of the pulse stress sequence. We have further examined the effect of frequency of the stressing voltage in the case in which measurement is made immediately following the stressing part of the final pulse (Fig. 1b). The data is shown in Fig. 7 for both modes of measurement (Figs. 1b and 1c). Again the modeling predicts almost no frequency dependence, in agreement with experiments we have performed over the frequency range 10 Hz – 10 kHz for the method measuring immediately following the relaxation part of the final cycle. However, if one measures following a stress cycle (Fig. 1b), there is a measurable frequency dependence. This difference is due to the growth of the recoverable term during the last cycle of the pulse train used in stressing. This is why at 10 kHz there is almost no difference between measuring ΔV_{th} after stress or after recovery, whereas at 10 Hz there is a considerable difference.

VI. Conclusions

New modeling and experimental measurements of the duty cycle effect on NBTI were completed for the case of SiON gate dielectric p-channel MOSFETs. The modeling predicts the functional dependence of the NBTI-induced threshold voltage shift on duty cycle and frequency of the stressing voltage. Although the data can be modeled using an approximate formalism, [7] a more physically correct model for the tunneling induced charging/discharging of recoverable charged defects in the gate insulator is still required. In a sense, the need to adapt the existing model [7] to explain the experimental charging/discharging results is further evidence for the approximate nature of its applicability.

Acknowledgment

The work performed by K. Kambour was supported by the U.S. Air Force under a contract sponsored, monitored, and managed by United States Air Force Air Force Material Command, Air Force Research Laboratory, Space Vehicles Directorate, Kirtland Air Force Base, N.M. 87117-5776.

Duc Nguyen's and Camron Kouhestani's work is sponsored by the Air Force Research Laboratory under agreement number FA9453-08-2-0259

References

[1] Mahapatra, S.; Islam, A.E.; Deora, S.; Maheta, V.D.; Joshi, K.; Jain, A.; Alam, M.A., "A critical re-evaluation of the usefulness of R-D framework in predicting NBTI stress and recovery," Proc. IRPS, 2011, pp. 614-620.

[2] B. Kaczer, T. Grasser, J. Franco, M. Toledano Luque, P. J. Roussel, and G. Groeseneken, "Recent trends in bias temperature instability,"J. Vac. Sci. Technol. B 29, 01AB01 (2011).

[3] V. Huard, C. Parthasarathy, N. Rallet, C. Guerin, M. Mammase, D. Barge, and C. Ouvrard, "New characterization and modeling approach for NBTI degradation from transistor to product level", Proc.IEDM, 2007, pp. 797–800.

[4] V. Huard, "Two independent components modeling for Negative Bias Temperature Instability," Proc. IRPS (2010), pp. 33-42.

[5] K. Kambour et al, in Proc. ICDIM (2012), in publication

[6] T. Grasser, B. Kaczer, T. Aichinger, W. Gös, and M. Nelhiebel, "Defect creation stimulated by thermally activated hole trapping as the driving force behind negative biastemperature instability in SiO2, SiON, and high-k gate stacks," in IIRW (2008), pp. 91-94

[7] T. L. and H.-S. Lee, "Characterization Modeling and Minimization of Transient Threshold Voltage Shifts in MOSFETs," IEEE J. Solid-State Circuits, vol. SC-29, pp. 239-252, March, 1994

[8] A. Islam, "Theory and characterization of random defect formation and its implication in variability of nanoscale transistors" PhD Thesis, Purdue University, 2010